This is the accepted manuscript made available via CHORUS. The article has been published as:

Impact of shell structure on the fusion of neutron-rich mid-mass nuclei

Varinderjit Singh, J. E. Johnstone, R. Giri, S. Hudan, J. Vadas, R. T. deSouza, D. Ackermann, A. Chbihi, Q. Hourdille, A. Abbott, C. Balhoff, A. Hannaman, A. B. McIntosh, M. Sorensen, Z. Tobin, A. Wakhle, S. J. Yennello, M. A. Famiano, K. W. Brown, C. Santamaria, J. Lubian, H. O. Soler, and B. V. Carlson

Phys. Rev. C **104**, L041601 — Published 13 October 2021

DOI: 10.1103/PhysRevC.104.L041601

Impact of shell structure on the fusion of neutron-rich mid-mass nuclei

Varinderjit Singh, J.E. Johnstone, R. Giri, S. Hudan, J. Vadas, and R. T. deSouza*
Department of Chemistry and Center for Exploration of Energy and Matter, Indiana University 2401 Milo B. Sampson Lane, Bloomington, Indiana 47408, USA

D. Ackermann and A. Chbihi
GANIL, CEA/DRF-CNRS/IN2P3, Bvd. Henri Becquerel, F-14076 Caen CEDEX, France

Q. Hourdille
Normandie Université, Unicaen, Caen, France

A. Abbott, C. Balhoff, A. Hannaman, A.B. McIntosh, M. Sorensen, Z. Tobin, A. Wakhle, and S.J. Yennello
Cyclotron Institute Texas A&M University, College Station, Texas 77843 USA

M.A. Famiano
Department of Physics Western Michigan University, Kalamazoo, Michigan 49008, USA

K.W. Brown and C. Santamaria
National Superconducting Cyclotron Laboratory, Michigan State University, East Lansing, Michigan 48824

J. Lubian and H.O. Soler
Instituto de Física, Universidade Federal Fluminense, Niteri 24210-340, R.J., Brazil

B. V. Carlson
Departamento de Fisica, Technologico da Aeronautica, Centro Tecnico Aerospacial, 12228-900 Sao Jose dos Campos, São Paulo, Brazil

(Dated: October 5, 2021)

The influence of shell effects on fusion of mid-mass nuclei is explored using isotopic chains of K and Ar ions on an oxygen target. Comparison of the reduced excitation functions reveals that the fusion cross-section for the open neutron-shell projectile nuclei ^{41}K and ^{45}K is systematically larger than for the closed neutron-shell projectiles ^{39}K and ^{47}K. The São Paulo fusion model using matter densities from systematics fails to describe the measured excitation functions. Use of more realistic densities from a Dirac-Hartree-Bogoliubov (DHB) approach performs significantly better though it still overpredicts the closed-shell nuclei.

PACS numbers: 21.60.Jz, 26.60.Gj, 25.60.Pj, 25.70.Jj

INTRODUCTION

Fusion of two heavy-ions is a fascinating process in which two strongly-interacting quantum systems merge, lose their individual identity, and assume a new identity. While the importance of shell structure in nuclei determines masses [1] and thus many conspicuous observables, its importance in, and influence on, heavy-ion fusion is less clear. As nuclei become neutron-rich their ground-state nuclear structure is modified by shell quenching [2] and the emergence of new "magic numbers"[3]. Recently, systematic examination of fusion for isotopic chains of carbon and oxygen nuclei on a carbon target [4, 5] has revealed a significant increase in the average above-barrier fusion cross-section for neutron-rich nuclei with an unpaired neutron. Whether this latter observation is confined only to light nuclei with an unpaired neutron is presently an open question. Radioactive beam facilities now provide the means to systematically investigate the impact of structure on fusion for isotopic chains extended to exotic neutron-rich nuclei [6–8].

Neutron-rich nuclei with extended density distributions exhibit larger fusion cross-sections. The cross-section can be additionally increased by intrinsic and collective excitation. At small excitation, a coupled-channel approach has been successful in describing the fusion of nuclei [9–11]. Despite this success of coupled-channel calculations, for neutron-rich nuclei with loosely bound valence neutrons one might expect additional neutron dynamics to emerge. Such dynamics can be theoretically probed through time-dependent approaches such as time-dependent Hartree-Fock [12] or density functional theory [13].

The simplest approach to calculating the fusion cross-section involves a double-folding of the density distribution with the assumption that the initial density distributions are frozen [14, 15]. The density distribution utilized is not restricted to a one-body description but can

include two-body or higher correlations allowing nuclear structure to influence the fusion cross-section. For near-barrier collisions, the critical point in fusion is the saddle point in the potential energy surface. Whether nuclear structure effects influence the fusion cross-section depends on whether they persist at the saddle point.

In the present work we examine the fusion of the neutron-rich nuclei at the N=20 and N=28 closed shells as well as open-shell nuclei by studying the fusion of ^{39,41,45,47}K+^{16}O and ^{36,44}Ar +^{16}O. The K isotopic chain was chosen based on the availability of these beams at the ReA3 accelerator facility at Michigan State University. The double closed-shell for ^{16}O provided a well-bound nucleus as the target enabling a systematic measurement of the impact of the projectile's shell structure on the fusion cross-section.

EXPERIMENTAL TECHNIQUE

Radioactive beams of K and Ar ions were produced by colliding ^{48}Ca beams at 140 A.MeV with a Be production target at the coupled-cyclotron facility at MSU-NSCL. The resulting reaction products were filtered by the A1900 spectrometer before being thermalized in a gas stopper. They were subsequently extracted from the gas stopper, charge bred to a high-charge state, and accelerated by the ReA3 linac before being transported to the experimental setup. For the stable isotopes, an ion source directly fed the charge breeder. Details on the experimental setup have been previously published [16] and are briefly summarized below.

The identity of ions incident on the target was measured particle-by-particle by using two microchannel-plate detectors (MCP) spaced ≈1.3 m apart together with two intervening axial-field ionization detectors. With these detectors a ΔE-TOF measurement was performed for each ion incident on the target. Measurement of the ΔE-TOF allowed rejection of beam contaminants. The electron emission foil of the downstream MCP detector also served as the target in the experiment. The intensities of the K and Ar beams incident on the target ranged between 1.0 x 10^4 (^{44}Ar/s) and 4.5 x 10^4 (^{39}K/s).

The ^{16}O target used was produced by evaporating ^{28}Si in a vacuum of 1x10^{-6} Torr. Under these conditions the deposited Si exhibited a significant oxygen content. The oxygen content in the target was measured by a Rutherford Backscattering measurement (RBS) and confirmed using X-ray Photoelectron spectroscopy [17]. This RBS measurement revealed an oxygen thickness of 98 ± 4 μg/cm^2 along with a Si thickness of 258 ± 10 μg/cm^2.

Fusion products were identified using an energy/time-of-flight (ETOF) approach. Fusion of K (Ar) ions with the ^{16}O target results in a compound nucleus of Co (Fe) with an excitation of ≈40-50 MeV. In contrast, fusion of the K (Ar) ions with the ^{28}Si nuclei produces a compound nucleus of Ge (As). Following de-excitation of the compound nucleus via emission of neutrons, protons and α particles, the resulting evaporation residue (ER) reflects the initial mass difference. Reactions on ^{16}O are thus distinguished on the basis of the mass of the ER by detecting it in annular Si detectors that subtend the angular range $1.0^\circ < \theta_{lab} < 7.3^\circ$. Evaporation residues were identified using the energy deposit in the Si detectors together with the time-of-flight between the downstream MCP detector and a Si detector [16].

The fusion cross-section, σ_F is extracted from the measured yield of ERs through the relation $\sigma_F = N_{ER}/(\epsilon_{ER}$ x t x $N_I)$ where N_I is the number of beam particles of a given type incident on the target, t is the target thickness, ϵ_{ER} is the detection efficiency, and N_{ER} is the number of evaporation residues detected. The number N_I is determined by counting the particles with the appropriate time-of-flight between the two MCPs that have the correct identification in the ΔE-TOF map. The measured target thickness was used. The number of detected residues, N_{ER}, is determined by summing the number of detected residues identified by the ETOF technique. Uncertainty in identifying an ER associated with fusion on ^{16}O is reflected in the error bars presented. To obtain the detection efficiency, ϵ_{ER}, a statistical model was used to describe the de-excitation of the fusion product together with the geometric acceptance of the experimental setup. The detection efficiency varied between ≈ 82-83% over the entire energy range. The statistical uncertainties of the measurement dominate the error bars shown. The second-largest contribution to the total uncertainty in the cross-section is due to the target thickness and is 4%.

Presented in Fig. 1a are the fusion excitation functions for ^{39,45,47}K + ^{16}O. As expected, based on the presence of eight additional neutrons, ^{47}K exhibits a larger fusion cross-section than ^{39}K. The additional neutrons in ^{47}K should not only correspond to a larger size for the nucleus (cross-section) but should also be associated with a stronger attractive potential moving the excitation function towards lower $E_{c.m.}$. Interestingly, ^{45}K has an even larger cross-section than ^{47}K despite having two fewer neutrons. Without consideration of shell effects one might expect that fewer neutrons should result in a weaker attractive potential and consequently a diminished fusion cross-section.

In Fig. 1b the fusion excitation functions for ^{36,44}Ar are examined. This comparison also involves a difference of eight neutrons as in the case of ^{39,47}K but does not involve the closed shells of N=20 and N=28. For $E_{c.m.}$ < 26 MeV the neutron-rich ^{44}Ar exhibits a larger cross-section. For $E_{c.m.}$ > 26 MeV however the cross-section is essentially the same for ^{44}Ar and ^{36}Ar.

To account for the difference in cross-section associated with a projectile nucleus having more neutrons the reduced excitation functions are compared in Fig. 2. The fusion cross-section σ_F has been scaled by the quantity

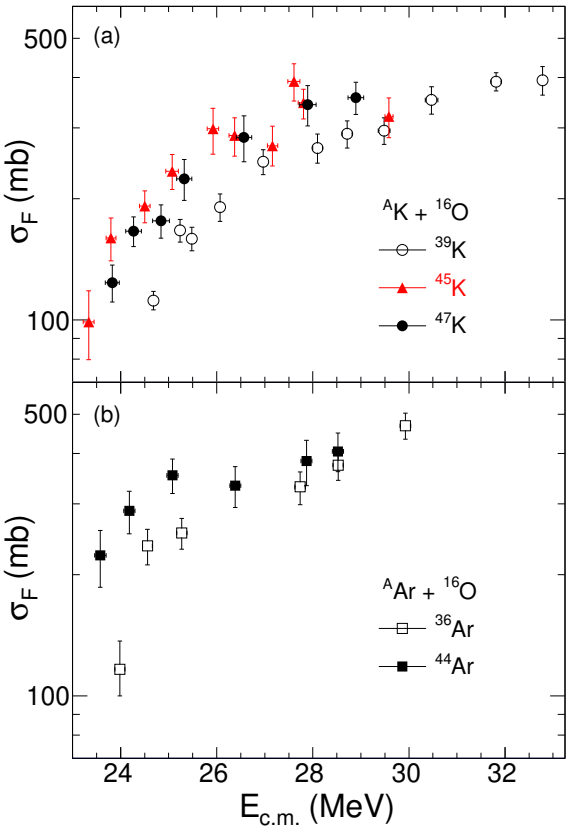


FIG. 1. Comparison of the fusion excitation functions for ^{39,45,47}K (upper panel) and ^{36,44}Ar (lower panel).

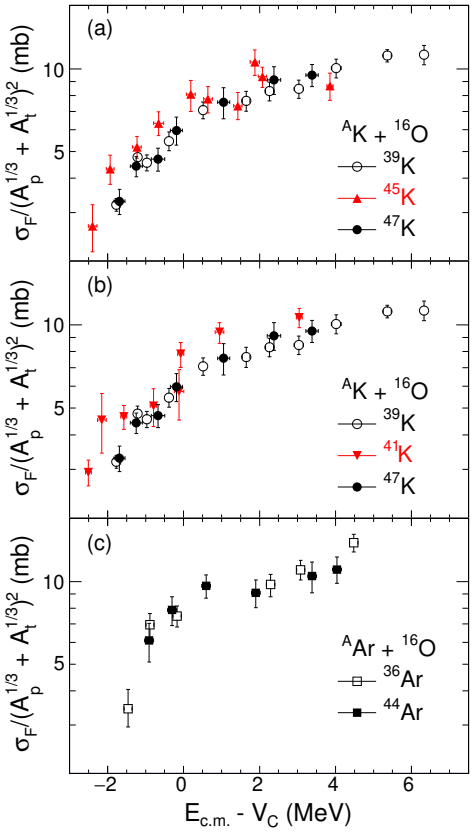


FIG. 2. Comparison of the reduced fusion excitation functions for ^{39,41,45,47}K and ^{36,44}Ar on a ^{16}O target.

$(A_P^{1/3} + A_T^{1/3})^2$ and its dependence on the incident energy is examined relative to the Coulomb barrier. The Coulomb barrier, V_C, is taken as V_C=1.44$Z_P Z_T/(A_P^{1/3} + A_T^{1/3})$. This scaling accounts for the systematic size and Coulomb barrier effects expected. This simple accounting of the Coulomb barrier does not include dependence of the charge radii on neutron number for the potassium isotopes recently reported [18]. Use of the simple prescription suffices as significant interpenetration of the charge distribution would be required for the impact of changes in the charge distribution to be manifested. When compared in this manner, ^{39}K and ^{47}K with their closed N=20 and N=28 shells exhibit essentially the same reduced fusion cross-section. This indicates that the increased cross-section for ^{47}K as compared to ^{39}K is effectively due to the larger ground-state size of the ^{47}K nucleus. In contrast to this result, a larger reduced fusion cross-section is evident for fusion of the open-shell ^{45}K (N=26). Thus, the systematic $A^{1/3}$ increase in size does not explain the ^{45}K fusion cross-section. It is interesting to note that this increased cross-section occurs close to and below the barrier. For 0 $\leq(E_{c.m.}$-$V_C)\leq$2 MeV, one observes a suppression in the reduced fusion cross-section. Similar structure in fusion excitation functions has been associated with resonance behavior in lighter systems [19]. The highest energy point for ^{45}K is consistent with the reduced cross-section of ^{39}K and ^{47}K, well below the expectation based upon extrapolation the reduced cross-section from lower energies.

The reduced excitation function for ^{41}K is compared with those of the closed-shell ^{39,47}K nuclei in Fig. 2b. As in the case of ^{45}K, the reduced fusion excitation function for ^{41}K is larger than that of the closed-shell nuclei. Remarkably, the presence of just two neutrons beyond the closed N=20 shell is sufficient to cause this increase.

In Fig. 2c the reduced fusion excitation functions for ^{36}Ar and ^{44}Ar are presented. For these nuclei the reduced excitation functions are essentially the same within the measurement uncertainties. The similarity of the reduced excitation functions for ^{39}K and ^{47}K, two closed-shell nuclei, or ^{36}Ar and ^{44}Ar, two open-shell nuclei, demonstrates the effectiveness of the reduced excitation function in accounting for the systematic size effect on fusion due to addition of neutrons in an isotopic chain. The difference observed in the reduced excitation function for ^{41}K and ^{45}K in comparing an open-shell with two closed-shell nuclei is therefore significant. It is essential to note that this comparison is valid when none of the analyzed isotopes exhibit large collectivity. Although some of the nuclei presented are neutron-rich, they are not weakly-

bound nuclei. Consequently, the fusion cross-sections are not affected by either the breakup channel or collectivity of these nuclei in the energy region investigated.

COMPARISON WITH THEORETICAL MODELS

The simplest description of fusion is through the interaction of the density distributions of the two interacting nuclei. If the interaction between the nuclei is non-adiabatic (i.e. described by the sudden approximation) it is sufficient to consider the ground-state density distributions. In the case of adiabatic collisions, collective modes in the colliding nuclei can be excited and need to be considered. Inclusion of these modes in a coupled-channels (CC) formalism results in an increase in the fusion cross-section at energies near and below the Coulomb barrier [20–22]. To investigate whether the observed fusion excitation functions can be described by the interaction of the ground-state density distributions of the projectile and target nuclei, the São Paulo model was used. The São Paulo potential [23] is a local-equivalent double folding of the projectile and target matter densities on the zero-range interaction multiplied by a strength coefficient e^{-4v^2/c^2} where v is its relative velocity and c is the speed of light. At energies near the Coulomb barrier this strength correction is insignificant. The São Paulo potential systematic [24] is the potential associated with matter densities described by a two-parameter Fermi-Dirac distribution with radius $R_0 = (1.31A^{1/3} - 0.81)$ fm and matter diffuseness $a = 0.56$ fm. This systematic was derived from the available experimental data for the charge distributions extracted from electron scattering and Dirac-Hartree Bogoliubov (DHB) calculations for many nuclei. As such it provides a general description in which structural effects have been averaged over. The São Paulo Potential systematic was used for the real part of the optical potential with a Woods-Saxon form used for the imaginary part with a depth of 50.0 MeV, reduced radius of 1.06 fm, and diffuseness of 0.20 fm for the one-channel calculations. Such a potential has been used in many CC calculations and their results successfully compare with experimental data [25–28].

Presented in Fig. 3 (dashed lines) are the predicted matter density distributions for the K and Ar isotopes, using the São Paulo potential systematic. All these distributions have a smooth Fermi-Dirac shape with a central density of ≈0.16 nucleons/fm^3. These smooth distributions reflect, in essence, the one-body mean-field nature of the nuclei considered and do not manifest nuclear structure associated with two-body correlations.

To calculate more accurate matter density distributions which include two-body correlations we performed Dirac-Hartree-Bogoliubov (DHB) calculations [29]. The correlations in the DHB calculations of the present work are limited to surface-pairing correlations. These correlations can make subtle modifications to the nuclear surface, extending and modifying the nuclear density. The details of these mean-field calculations using an axially-symmetric self-consistent approximation are reported in Ref. [30]. The resulting matter distributions are shown in Fig. 3 as the solid lines. Evident in the DHB matter distributions is a double-humped structure, a manifestation of the shell structure. For ^{39}K the dominant peak is located at lower values of R. With increasing neutron number the density of this inner peak decreases until at ^{47}K the outer peak is the dominant peak in density. A similar trend is observed between ^{36}Ar and ^{44}Ar although for these nuclei the inner peak remains the larger peak. As the fusion of two nuclei is typically viewed as sensitive to the tails of the matter distribution, an expanded view of this region is shown in the insets of Fig. 3. It is noteworthy that the tails of the matter distributions are quite similar although the DHB distributions are *slightly* less extended than the systematics.

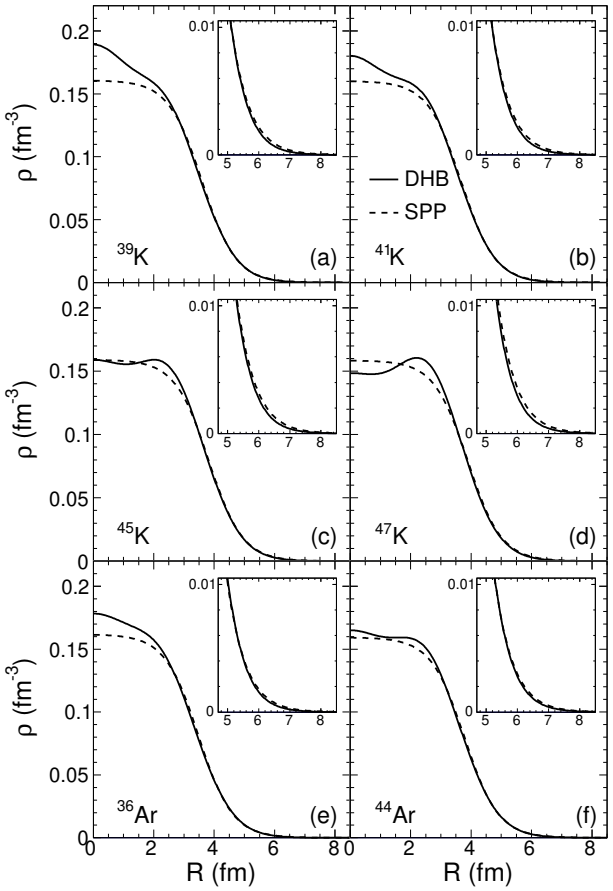


FIG. 3. Comparison of the matter density distributions given by the systematics that is typically used within the São-Paulo fusion model with the density distributions predicted by Dirac Hartree Bogoliubov (DHB) calculations. Shown in the insets are the tails of the matter distributions.

Displayed in Fig. 4 are the proton and neutron density distributions predicted by the DHB model. One observes

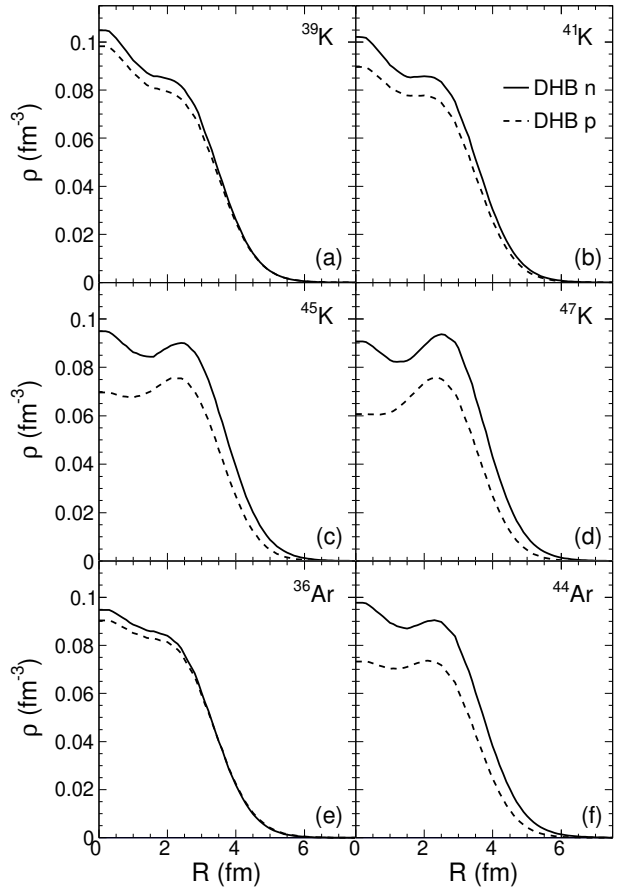


FIG. 4. Density distributions of protons (dashed) and neutrons (solid) for K and Ar isotopes predicted by the DHB calculations.

that addition of neutrons to ^{39}K influences not only the neutron but also significantly impacts the proton density distribution. As the peak in neutron density situated at large R increases in magnitude, the proton peak situated at large R also increases in magnitude. As the total number of protons is constant, this increase is correlated with a decrease in the value of the central proton density. This outward displacement of the proton density by additional neutrons can be thought of as the resistance of nuclei to polarization of the ground state. This behavior has previously been noted in relativistic mean-field calculations for neutron-rich oxygen isotopes and reflects the n-p interaction via the strong force [31]. Close examination of this outward pull of the valence neutrons on the core (N$\leq$20) neutrons as compared to the core protons reveals that the protons experience a larger outward pull. This difference can be interpreted as a repulsion between the valence neutrons and the core neutrons due to the Pauli exclusion principle. Similar behavior is also observed for the Ar isotopes.

Using the DHB matter distributions for both the projectile and ^{16}O target nuclei, the São Paulo Potential was generated and used to calculate the fusion cross-section. The theoretical predictions are compared with the experimental data in Fig. 5. In addition to the cross-sections resulting from the DHB matter densities (solid lines) the cross-sections associated with the systematics densities are also shown (dashed lines). In all cases use of the DHB densities results in a significant reduction of the fusion cross-section as compared to the systematics. This reduction is apparent over the entire energy interval considered. The similarity of the tail of the density distribution for both the DHB and systematics suggests that the change in the cross-section is due to the difference in the interior part of the density distribution. Further theoretical work to reproduce these data are needed to confirm this conclusion.

Comparison of the theoretical predictions with the experimental excitation functions is revealing. For the open neutron-shell isotopes ^{41,45}K, the theoretical model with the DHB densities provides a reasonable prediction of the excitation function particularly for the lower energies. However, in the case of the closed neutron-shell ^{47}K and particularly for ^{39}K, the model overpredicts the measured cross-sections. This overprediction for the case of the closed-shell nuclei might suggest that the ground-state configurations at the saddle point that result in fusion are more compact than the ground-state DHB calculations indicate. Alternatively, it might signal that higher order correlations, not present in the DHB calculations are more important for these closed neutron-shell nuclei. In the case of the ^{36,44}Ar nuclei the agreement is intermediate between that of the open-shell and closed-shell K isotopes.

The fact that the São-Paulo fusion model using the DHB densities *overpredicts* the experimental data is also significant. Coupling to low-lying collective modes acts to increase the fusion cross-section. Given that the ground-state calculation already overpredicts the measured cross-section, the excitation of low-lying collective modes can be ruled out. The largest discrepancy is observed for the closed neutron-shells at N=20 and N=28. Presumably these closed-shell nuclei are the least likely to undergo collective excitations. The persistence of shell effects at the saddle point reflects the low intrinsic excitation of the saddle configuration.

CONCLUSIONS

Systematic measurement of the fusion excitation functions for ^{39,41,45,47}K + ^{16}O and ^{36,44}Ar + ^{16}O has yielded surprising results. The open neutron-shell nuclei of ^{41,45}K manifest larger reduced fusion cross-sections than the closed neutron-shell isotopes ^{39,47}K. This result indicates that the additional binding due to the closed shell structure is present at the saddle point. In all cases considered, the São Paulo fusion model using the systematic densities overpredicts the measured fusion cross-sections.

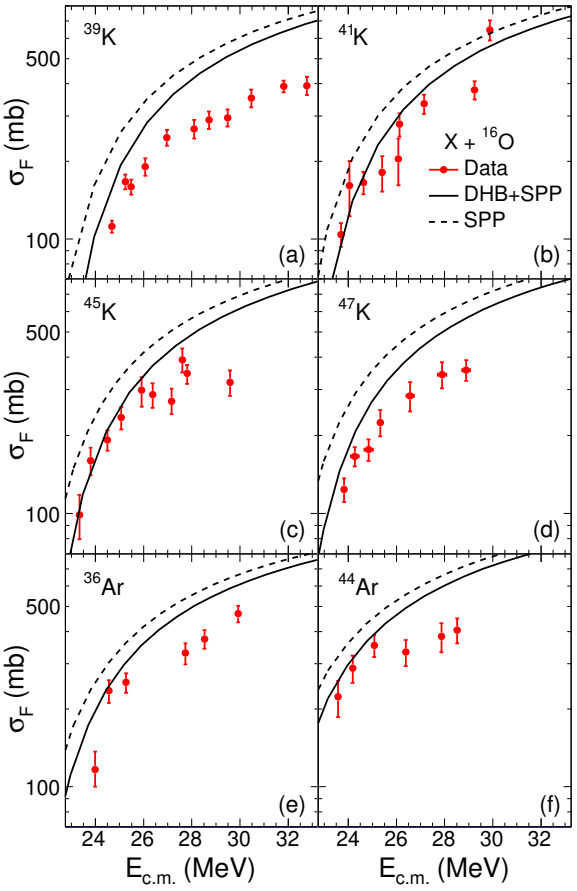


FIG. 5. Comparison of the experimental cross-sections with the predictions of the São Paulo model using DHB densities as well as densities from systematics.

Use of more realistic density distributions from a Dirac-Hartree-Bogoliubov (DHB) calculation resulted in a reduction of the predicted fusion cross-section as compared to the systematics. For the open-shell nuclei, the use of these more accurate ground-state densities in the São Paulo fusion model provided a reasonable description, particularly for the K isotopes. For the closed-shell nuclei however use of the DHB densities still overpredicts the measured cross-sections particularly above the barrier. This result emphasizes the importance understanding shell effects at the saddle point to achieve an accurate description of fusion.

We acknowledge the high quality beams provided by the staff at NSCL, Michigan Sate University that made this experiment possible. This work was supported by the U.S. Department of Energy Office of Science under Grant Nos. DE-FG02-88ER-40404 (Indiana University), DE-FG02-93ER-407773 (Texas A&M University) and the National Science Foundation under PHY-1712832. One of us (Q.H.) was supported by CNRS and the Region of Normandy (Région Normandie), France. One of us (D.A.) is supported by the European Commission in the framework of CEA-EUROTALENT 2014-2018 (noPCOFUND-GA-2013-600382). Brazilian authors acknowledge partial financial support from CNPq, FAPERJ, FAPESP, CAPES and INCT-FNA (Instituto Nacional de Ciência e Tecnologia- Física Nuclear e Aplicações) Research Project No. 464898/2014-5

* desouza@indiana.edu

[1] S. C. Pieper, Nucl. Phys. A **751**, 516 (2005).
[2] P. Doornenbal *et al.*, Phys. Rev. Lett. **111**, 212502 (2013).
[3] I. T. R. Kanungo and A. Ozawa, Phys. Lett. B **528**, 58 (2002).
[4] S. Hudan, R. T. deSouza, A. S. Umar, Zidu Lin, and C. J. Horowitz, Phys. Rev. C **101**, 061601 (2020).
[5] R. T. deSouza *et al.*, Physs. Lett. B **814**, 136115 (2021).
[6] NSCL, National Superconducting Cyclotron Laboratory, Michigan State University, USA.
[7] GANIL, Grand Accelérateur National d'Ions Lourds, Caen, France.
[8] FRIB, Facility for Rare Isotope Beams, Michigan State University, USA.
[9] G. Montagnoli and A. Stefanini, Rev. Mod. Phys. **53**, 169 (2017).
[10] B. Back, H.Esbensen, C. Jiang, and K. Rehm, Rev. Mod. Phys. **86**, 317 (2014).
[11] C. Jiang, B. Back, H. Esbensen, R. Janssens, S. Misicu, K. Rehm, P. Collon, C. Davids, D. Henderson, L. Jisonna, S. Kurtz, C. Lister, M. Notani, M. Poaul, R. Pardo, D. Peterson, D. Seweryniak, B. Shumard, X. Tang, I. Tanihata, X. Wang, and S. Zhu, Physics Letters B **640**, 18 (2006).
[12] A. S. Umar, V. E. Oberacker, and C. J. Horowitz, Phys. Rev. C **85**, 055801 (2012).
[13] R. Furnstahl, Nuclear Physics News **21**, 18 (2011).
[14] L. R. Gasques, L. C. Chamon, D. Pereira, M. A. G. Alvarez, E. S. Rossi, C. P. Silva, and B. V. Carlson, Phys. Rev. C **69**, 034603 (2004).
[15] L. R. Gasques, A. Afanasjev, M. Beard, M. J. Lubian, T. Neff, M. Wiescher, and D. Yakolev, Phys. Rev. C **76**, 045802 (2007).
[16] J. Vadas, V. Singh, B. B. Wiggins, J. Huston, S. Hudan, R. T. deSouza, Z. Lin, C. J. Horowitz, A. Chbihi, D. Ackermann, M. Famiano, and K. W. Brown, Phys. Rev. C **97**, 031601(R) (2018).
[17] J. Johnstone *et al.*, Nucl. Instr. Meth. A **953**, 163267 (2020).
[18] A. Koszorus *et al.*, Nature Physics **17**, 439 (2021).
[19] A. D. Frawley, N. R. Fletcher, and L. C. Dennis, Phys. Rev. C **25**, 860 (1982).
[20] M. Beckerman, M. Salomaa, A. Sperduto, H. Enge, J. Ball, A. DiRienzo, S. Gazes, Y. Chen, J. D. Molitoris, and M. Nai-feng, Phys. Rev. Lett. **45**, 1472 (1980).
[21] R. G. Stokstad and E. E. Gross, Phys. Rev. C **23**, 281 (1981).
[22] D. Abriola, D. DiGregorio, J. E. Testoni, A. Etchegoyen, M. C. Etchegoyen, J. O. Fernández Niello, A. M. J. Ferrero, S. Gil, A. O. Macchiavelli, A. J. Pacheco, and J. Kittl, Phys. Rev. C **39**, 546 (1989).

[23] L. C. Chamon, D. Pereira, M. S. Hussein, M. A. Cândido Ribeiro, and D. Galetti, Phys. Rev. LettC. **79**, 5218 (1997).

[24] L. C. Chamon, B. V. Carlson, L. R. Gasques, D. Pereira, C. De Conti, M. A. G. Alvarez, M. S. Hussein, M. A. Cândido Ribeiro, E. S. Rossi, and C. P. Silva, Phys. Rev. C **66**, 014610 (2002).

[25] G. S. Li, J. G. Wang, J. Lubian, H. O. Soler, Y. D. Fang, M. L. Liu, N. T. Zhang, X. H. Zhou, Y. H. Zhang, B. S. Gao, Y. H. Qiang, S. Guo, S. C. Wang, K. L. Wang, K. K. Zheng, R. Li, and Y. Zheng, Phys. Rev. C **100**, 054601 (2019).

[26] M. Fisichella, A. C. Shotter, P. Figuera, J. Lubian, A. Di Pietro, J. P. Fernandez-Garcia, J. L. Ferreira, M. Lattuada, P. Lotti, A. Musumarra, M. G. Pellegriti, C. Ruiz, V. Scuderi, E. Strano, D. Torresi, and M. Zadro, Phys. Rev. C **95**, 034617 (2017).

[27] L. Canto, P. Gomes, R. Donangelo, J. Lubian, and M. Hussein, Physics Reports **596**, 1 (2015).

[28] L. Canto, P. Gomes, R. Donangelo, and M. Hussein, Physics Reports **424**, 1 (2006).

[29] B. V. Carlson and D. Hirata, Phys. Rev. C **62**, 054310 (2000).

[30] L. Chamon, B. Carlson, and L. Gasques, Computer Physics Communications **267**, 108061 (2021).

[31] C. Horowitz, Private Communication.